Kinetics of chronic lymphocytic leukemia cells in tissues and blood during therapy with the BTK inhibitor ibrutinib

Dominik Wodarz, Naveen Garg, Natalia L. Komarova, Ohad Benjamini, Michael J. Keating, William G. Wierda, Hagop Kantarjian, Danelle James, Susan O'Brien, Jan A. Burger

Supplementary Materials 1: Patients and data

Patient characteristics

To characterize the dynamics of CLL cell tissue redistribution during therapy with ibrutinib, we analyzed a cohort of previously treated patients that received single-agent ibrutinib at a dose of 420 MG continuously daily on a Phase 1/2 clinical trial (PCYC-1102-CA) at MD Anderson Cancer Center between 2010 and 2012. The clinical details of these patients are summarized in Table 1A, main text. Only ten patients of this cohort were used for this analysis because besides determining the absolute lymphocyte counts (ALC) in the blood, the volume of lymph nodes and spleen was quantified by radiological measurements. The radiological data are crucial for our calculations and were only available in the selected patients.

Tissue volumetric analysis

The volume of lymphoid tissues and the spleen was quantified by computed tomography (CT) scans prior to therapy, and at two time points during ibrutinib therapy (specified for each patient in Table 1 of this Supplementary Material). Lymphoid tissue

volumes were calculated from CT scans using the following method: the 5 largest conglomerations of lymph nodes as well as the spleen were identified by visual inspection of the cases by a radiologist. A contour was hand drawn around the center CT slice containing each conglomerate of nodes. The average of the maximum and minimum axis diameters of the contoured region of interest was used to calculate an effective radius, and the spherical volume was calculated based on this radius.

The total number of cells in tissue was derived from the sum of measured tissue volumes, assuming that the average volume of a CLL cell is 166fl[1]. For enlarged lymph nodes, it was assumed that the majority of the volume was determined by the presence of CLL cells, since the size of healthy lymph nodes is small relative to the size of the enlarged tissue in the patients. Because the average size of the spleen in healthy individuals is not negligible compared to the size of the enlarged spleen, about 150 cubic centimeters[2], we subtracted this number from the volume of the enlarged spleen in the CLL patients in order to obtain the volume that is attributable to the presence of CLL cells. The total number of CLL cells in the tissues can be quantified accurately in this way before the start of treatment and at the first measurement during treatment. At the second CT scan measurement during treatment, lymph node volumes had already declined to near normal levels, thus not accurately reflecting the likely continued decline of the tumor cell population in tissue. Hence, while all blood measurements were used to fit the model to the data, only the first two data points in tissue were taken into account. Details about fitting are described in Supplementary Materials 2. We further note that the third point of tissue data could in principle be included, but this would require a significantly more complex model. The price of being able to include this extra

point is at least one additional parameter in the model, which would significantly reduce the certainty of the fits. Therefore, we adopted the simpler and more informative approach, see Supplementary Materials 2.

We note that tumor cell burden in the bone marrow was not quantified in this study. The main effect of not including bone marrow is to under-estimate the total number of CLL cells in the tissues. If bone-marrow was included, then the total tissue disease burden would be higher. Consequently, the percentage of cells that redistributed from tissue into the blood would be lower and the tissue death rate estimates might become higher. Hence, our basic message would not change on a qualitative level. It might be more pronounced than our calculations suggest. These arguments assume similar homing and redistribution kinetics for bone marrow and the other tissue sites.

Blood lymphocyte counts

The number of lymphocytes per microliter blood was measured directly by serial complete blood counts (CBC). However, this number is not commensurate with the estimated number of tissue cells, which are not given per volume, but for the whole body. Therefore, the number of lymphocytes per microliter blood was multiplied by the blood volume of each patient, estimated from the body weight[3]. This yielded the total number of lymphocytes in the whole blood, which was used in plots and model fits. We note that while for each patient, tissue tumor burden was quantified at 3 time points; many more data points are available for absolute lymphocyte counts in blood (Figure 1 in main text). The lymphocyte dynamics in the blood exhibited the typical dynamics

described previously[4]. Transient lymphocytosis was followed by a phase of decline until the number of cells stabilized at a level significantly lower than before therapy (Figure 1, main text). This was accompanied by a significant reduction in the volume of the lymphoid tissue involved by CLL, which typically did not appear enlarged anymore after 20 weeks of ibrutinib treatment (Supplemental Figure S1). The characteristics of the observed lymphocytosis in our patients are consistent with patterns that have been reported previously. Peak lymphocyte counts were reached on average 46.1±35.6 days after the initiation of ibrutinib therapy and were 5.2±3.5 fold higher than at baseline. Following the peak, the lymphocyte counts declined to <5000 cells per □l blood in 5 patients on average 346.8±67.3 days after treatment initiation. While in the rest of the patients significant declines in lymphocyte counts were observed after the peak, their counts remained above 5000 cells per □l blood for the duration for which the patients were followed.

Number of patients and limitations

Due to the required volumetric analysis, our patient pool was limited to ten patients. Although for each individual patient, our parameter estimates are robust because of the availability of many data points to which the model was fit (blood and tissue data were fitted simultaneously), statistics about the variation of parameter values among patients can be improved in future studies that examine larger patient populations. In this context, it will also be interesting to examine differences between patient sub-groups, such as IGHV mutated and unmutated patients.

References

1. Kuse, R., Schuster, S., Schubbe, H., Dix, S. & Hausmann, K. Blood lymphocyte volumes and diameters in patients with chronic lymphocytic leukemia and normal controls. *Blut* **50**, 243-248 (1985).
2. Eichner, E.R. Splenic function: normal, too much and too little. *Am J Med* **66**, 311-320 (1979).
3. Nadler, S.B., Hidalgo, J.H. & Bloch, T. Prediction of blood volume in normal human adults. *Surgery* **51**, 224-232 (1962).
4. Advani, R.H.*, et al.* Bruton tyrosine kinase inhibitor ibrutinib (PCI-32765) has significant activity in patients with relapsed/refractory B-cell malignancies. *J Clin Oncol* **31**, 88-94 (2013).

Patient	Measure 2, days post treatment initiation	Measure 3, days post treatment initiation
1	55	223
2	56	136
3	43	135
4	55	141
5	55	139
6	55	138
7	53	136
8	56	140
9	55	139
10	54	not taken

Supplementary Material1, Table S1: Days after treatment start at which tissue volumes were determined for individual patients. The first measure was taken prior to therapy. Measures 2 and 3 were taken on the days indicated in the table.

Kinetics of chronic lymphocytic leukemia cells in tissues and blood during therapy with the BTK inhibitor ibrutinib

D. Wodarz, N. Garg, N.L. Komarova, O. Benjamini, M.J. Keating, W.G. Wierda, H. Kantarjian, D. James, S. O'Brien, and J.A. Burger

Supplementary Materials 2

1 The mathematical model

The mathematical model that describes the dynamics of CLL lymphocytes is given by the following system of ordinary differential equations:

$$\dot{x} = -mx - d_1(x - c), \quad (1)$$

$$\dot{y} = mx - d_2 y, \quad (2)$$

$$x(0) = x_0, \quad (3)$$

$$y(0) = y_0. \quad (4)$$

Here, the time-dependent functions $x(t)$ and $y(t)$ stand for the numbers of CLL lymphocytes in tissue and blood respectively. Coefficient d_1 measures the cell death rate in tissue, and coefficient m the redistribution rate of cells from tissue to blood. It is convenient to introduce parameter $\alpha = m + d_1$, which is the sum of these two rates that measures the overall rate of decline of CLL lymphocytes in tissues (nodal decline). Coefficient d_2 describes the death rate of lymphocytes in blood. The quantities x_0 and y_0 are the initial (pre-treatment) values of the lymphocyte numbers in tissue and blood. The death rates can be used to calculate the average life-span of cells in tissue and blood. The death rate defines the reciprocal of the mean time until a typical cell dies, and this holds in the presence of redistribution from tissue to blood.

The parameter c is included to describe the decline of the lymphocytes towards a steady level, as observed. It is introduced such that the fit of the model is consistent with the data in the long term. The majority of the

patients do not achieve complete remissions. At present, the reason for the corresponding long-term stabilization of the lymphocyte counts in patients is unknown. Our model, therefore, does not predict the stabilization behavior as an "output", as a result of a specific biological mechanism. Instead, we simply use the fact of stabilization as an "input". The simplest way to do this is to introduce a single extra parameter, c, which accounts for this behavior. This parameter is found by fitting the model, along with the other parameters, as explained below. An alternative would be to include a hypothetical mechanism, which would explain the existence of the long-term stabilization of the lymphocyte counts. However, there is currently insufficient information available to robustly incorporate that into a mathematical modeling framework, and this is beyond the scope of the current manuscript.

Making the change of variables, $X = x - C_x$, $Y = y - C_y$, where $C_x = \frac{d_1}{m+d_1}c$ and $C_y = mC_x/d_2$, we have

$$\begin{aligned} \dot{X} &= -\alpha X, && (5)\\ \dot{Y} &= mX - d_2 Y, && (6)\\ X(0) &= x_0 - C_x, && (7)\\ Y(0) &= y_0 - C_y. && (8) \end{aligned}$$

The solution reads

$$\begin{aligned} x(t) &= C_x + (x_0 - C_x)e^{-\alpha t}, && (9)\\ y(t) &= \frac{mx_0}{d_2-\alpha}e^{-\alpha t} + \left(y_0 - \frac{mx_0}{d_2-\alpha} - C_y\right)e^{-d_2 t} + C_y. && (10) \end{aligned}$$

2 The relative number of cells redistributed from tissues to blood

An important quantity that we measure from the model is the ratio of the cells transferred from the tissues to the blood, to the initial number of cells in the tissues:

$$Z(t) = \frac{\int_0^t mx(t')\,dt'}{x_0} = \frac{m}{\alpha x_0}\left((x_0 - C_x)(1 - e^{-\alpha t}) + \alpha C_x t\right). \qquad (11)$$

In particular, if we had $C_x = 0$, then the expression simplifies to $Z = \frac{m}{\alpha}(1 - e^{-\alpha t})$. In the presence of $C_x > 0$, the quantity Z grows linearly in time in

the long term:

$$Z \to \frac{m}{\alpha}\left(1 + \frac{C_x}{x_0}(\alpha t - 1)\right).$$

This growth is a consequence of the presence of a remaining equilibrium level of CLL lymphocytes in tissues ($c > 0$), consistent with data. In order to design a reasonable measure of the number of cells redistributed from tissues to the blood in the course of treatment, we use the cut-off for the time-variable in equation (11),

$$T_c = \frac{1}{m + d_1} + \frac{1}{d_2}. \tag{12}$$

This quantity is a composite of two characteristic times of decay: the first term measures the decay-time of CLL lymphocytes in tissues (and it is defined by both redistribution and death processes), and the second term measures the decay time in blood, defined uniquely by the death rate d_2. (Normally, in the presence of a single exponential decay process, the characteristic time of decay is given by the inverse of the decay rate. In the presence of two such processes, one can either use the maximum of the two inverse decay rates, or their sum. While both measures give a similar order of magnitude for T_c, here we chose to use the second one (formula (12)) for its mathematical convenience.)

Patient	1	2	3	4	5	6	7	8	9	10
T_c, days	131.2	86.8	107.0	1132.4	136.5	194.2	214.3	464.2	137.5	319.8

Table 1: (Supplementary Materials 2.) The values of T_c, in days, calculated for the patients in the study.

In Table 1 (Supplementary Materials 2) we present the values of T_c calculated for the individual patients in this study by using formula (12) and the parameter values found by the fitting procedure. The details of the fitting procedure are explained in the next sections.

3 The fitting procedure

Fitting the number of CLL cells in blood and tissue. If only the blood cell counts were available, then it would not be possible to measure the quantity Z. The reasons are two-fold.

(i) From fitting $y(t)$ to the data, we can find the best fitting values of α, d_2, mx_0, y_0, and C_y. Note that one cannot find coefficients d_1, m, and x_0 separately from fitting this function, and only their combination $(m + d_1)x_0$ can be determined.

(ii) It turns out that apart from the solution just described, there is always a second solution which yields exactly the same fit, with

$$\hat{\alpha} = d_2, \quad \hat{d_2} = \alpha, \tag{13}$$

$$\hat{C_y} = C_y, \quad \hat{y_0} = y_0, \quad \hat{mx_0} = mx_0 + (y_0 - C_y)(d_2 - \alpha). \tag{14}$$

This duality of solution does not allow one to determine the parameters necessary to evaluate quantity Z.

Therefore, in order to quantify Z, we had to estimate the number of CLL cells in tissues.

The estimated number of CLL cells in tissues. The data that were fitted to solution (9-10) had the form $(\{t_i^n, y_i^n\}, \{\tau_k^n, x_k^n\})$, where the index $n = 1, \ldots, 10$ denotes the patient number. For each patient, n, the values y_i^n are the measured numbers of lymphocytes per microliter of blood, at times t_i^n with $i = 0, 1, \ldots, N_n$. The number of blood measurements for the 10 patients included in the study ranged from 12 to 40. The values x_k^n are the estimated numbers of CLL cells in tissue, at times τ_k^n, with $k \in \{0, 1\}$.

The total numbers of CLL cells in tissue comprise measurements in several compartments, see Supplementary Materials 1 for details. In order to capture the tissue dynamics better, we have performed a more detailed analysis of the data in different compartments. Let us enumerate the different compartments in patient n by the index $i = 0, 1, \ldots, N_n$, where the variable N_n ranges from 2 to 7, and $i = 0$ stands for the spleen. Accordingly, the measurements in the different compartments are denoted by $x_k^{n,i}$, and $x_k^n = \sum_{i=0}^{N_n} x_k^{n,i}$. As explained, the estimates for the numbers of CLL cells in tissues were derived from the volume measurements of the different organs.

The values x_1^n allow to characterize the decline of the number of CLL cells upon treatment. It has been observed that the spleen volume drops significantly less than the volume of other compartments. This is because healthy cells contribute significantly to the volume of the spleen. In order to include this information in the analysis and refine our estimates of the CLL cell numbers, we have performed the following:

(i) Because the average size of the spleen in healthy individuals is not negligible compared to the size of the enlarged spleen, about 150 cubic cm^2, we subtracted this number from the volume of the enlarged spleen in the CLL patients in order to obtain the volume that is attributable to the presence of CLL cells, as explained in Supplementary Materials 1. This is reflected in the value x_0^n that was used for fitting.

(ii) It was assumed that the drop in the spleen volume does not fully reflect the decrease in the number of CLL cells in this organ. In order to calculate the decline rate of CLL cells, for each patient we evaluated the decline rate averaged over the compartments (except for the spleen): $\tilde{r}^n = \frac{1}{N_n} \sum_{i=1}^{N_n} \frac{1}{\tau_1^n - \tau_0^n} \ln(x_0^{n,i}/x_1^{n,i})$. Then the estimated number of CLL cells in the tissue at point τ_1^n was refined by taking $x_1^n = x_0^n \exp(-\tilde{r}^n(\tau_1^n - \tau_0^1))$.

Parameter ranges. For each patient n, the data for the blood and for the tissue were fitted simultaneously, by using the following protocol. The six model parameters d_1, d_2, m, x_0, y_0, and c were classified into three groups:

- Parameters, whose value can roughly be estimated from the row data: x_0 and y_0. For these parameters, we roughly know the value, because $x_0 \approx x_0^n$ and $y_0 \approx y_0^n$. For the purposes of fitting, we allowed a certain degree of freedom in determining the actual value for these parameters, and thus varied them in a narrow range around their rough estimation:

$$x_0 \in [0.85x_0^n, 1.15x_0^n], \quad y_0 \in [0.85y_0^n, 1.15y_0^n].$$

  There are two reasons why a fitted parameter, x_0 or y_0, may be different from the actual measured value, x_0^n or y_0^n, for a given patient. (i) It has to be assumed that the clinical quantification of the absolute lymphocyte count may contain a certain level of error. Thus, if the absolute lymphocyte count at the start of treatment was measured, we allowed the model fit to vary this by 15%. For example, it is possible that the model fits the rest of the data points much better if it assumes an initial number of cells that is somewhat lower or higher than the measured one. (ii) In some patients, the first data point was not measured upon initiation of treatment, but up to 1 week after start of treatment. In this case, the true clinical number of cells at the start of treatment was unknown, which can lead to a more extensive discrepancy between

the initial cell number estimated in the model and the first measured clinical data point during treatment.

- Parameter with a data-derived upper bound: c. For this parameter, while we cannot extract its value from the data directly, we can find an upper bound by using the radiological data. Namely, we use the range

$$c \in [0, 80B_n],$$

where B_n is the blood volume for patient n (see Supplementary Materials 1). This choice of an upper bound reflects the fact that for all the patients in the dataset, the number of CLL cells in tissue in the long run was always below this level.

- Parameters that require fitting to estimate: d_1, d_2, and m. These model parameters were varied within a wide range. The ranges were chosen as follows:

$$d_1 \in [0.001, 0.1], \quad d_2 \in [0.001, 0.1], \quad m \in [0.0001, 0.5].$$

These ranges were determined after a preliminary implementation of the data fitting procedures with significantly wider ranges. This established the order of magnitude of the values into which the parameter estimates fall.

Finding the best fit. For each iteration step, we picked a parameter combination from a uniform distribution in the ranges above (in other versions of this algorithm, we varied the logarithm of the parameter values uniformly in an appropriate range). We then used solution (9-10) to create the theoretical values, $(x(\tau_k^n), y(t_i^n))$. The sums of squared errors were formed:

$$ssx_n = \sum_{k=0}^{1} (x_k^n - x(\tau_k^n))^2, \quad ssy_n = \sum_{i=0}^{N_n} (y_i^n - y(t_i^n))^2,$$

as well as the sums of squares (the square norm) of the data:

$$S_{x,n} = \sum_{k=0}^{1} (x_k^n)^2, \quad S_{y,n} = \sum_{i=0}^{N_n} (y_i^n)^2.$$

For the fixed parameter combination, the quantity

$$S_n = \frac{ssx_n}{S_{x,n}} + \frac{ssy_n}{S_{y,n}} \tag{15}$$

was calculated. This quantity (rather than the total sum of square errors) was minimized. This choice was motivated by two factors: (1) There were many time-points for the lymphocyte counts in the blood, and only two time-points where the tissue values were measured. (2) The two types of variables (the lymphocyte counts in blood and the estimated number of CLL cells in tissues) had different magnitudes. Therefore, we needed to normalize the two types of squared errors to make them commensurate. This choice is not unique, and we also tried alternative normalizations (e.g. when we add the square roots of the two fractions in (15)); this yielded very similar numerical results.

To minimize the quantity S_n, we calculated it for a random choice of parameters. Then another parameter combination was picked, and if the new value S_n was smaller than the previously found one, then S_n was replaced by the new value. This procedure was repeated 2×10^{12} times. As a result, a set of parameters was produced that minimized the quantity S_n. This was deemed the best fitting parameter combination.

As an alternative approach we also used a minimization procedure that utilized the steepest descent method to find a local minimum of the function S_n. The advantage of this procedure is its efficiency, and a disadvantage is the appearance of local minima. Because of the latter, this method had to be implemented many times, varying the initial guess for the parameters. The two procedures gave very similar numerical results.

Supplemental figures and tables

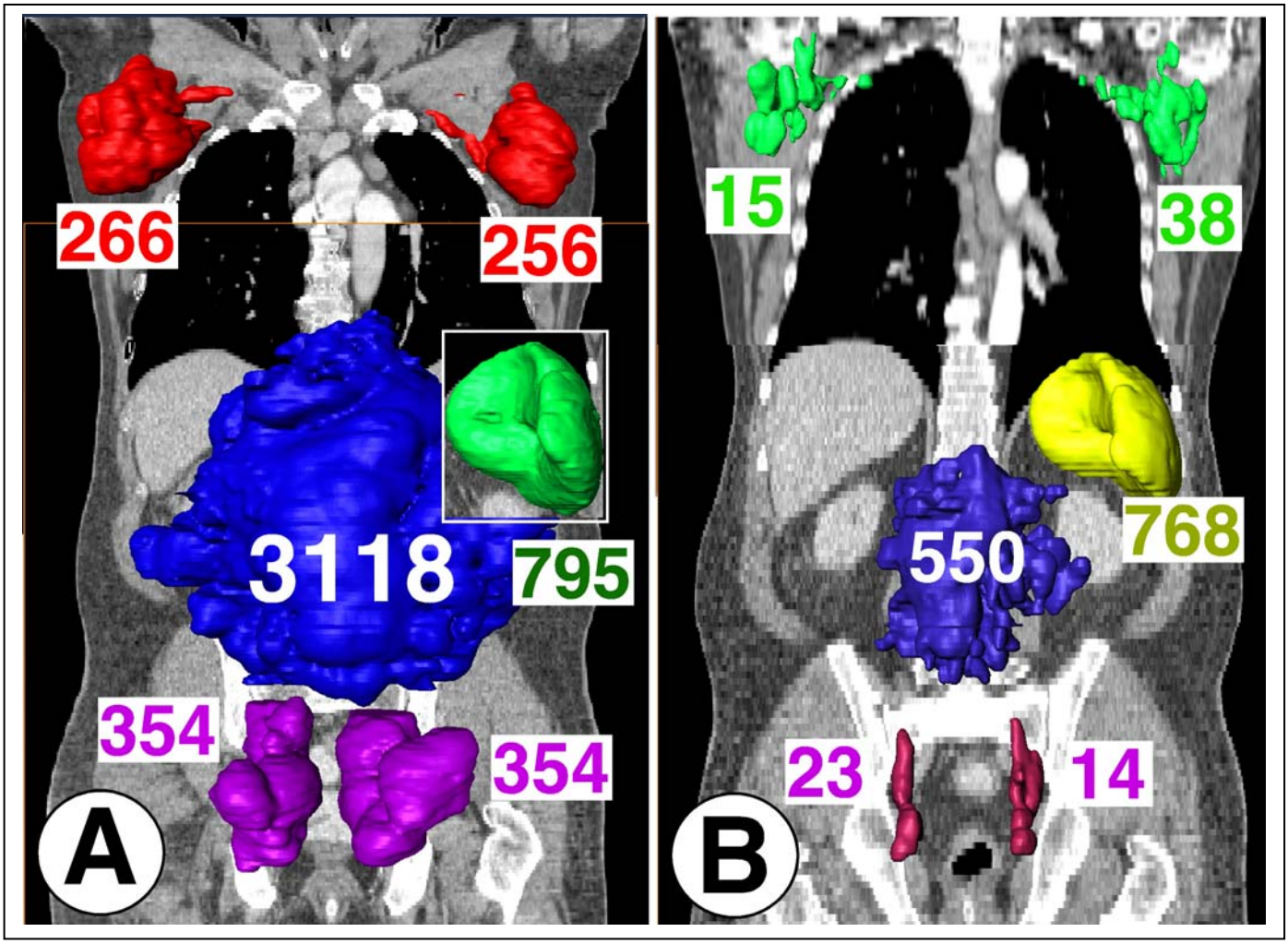

Figure S1 Volumetric analyses of CLL lymph node and spleen manifestation before (A) and (B) after 2 months of therapy with ibrutinib. Depicted are CT images from CLL patient #4 from our series with superimposed reconstruction of main areas of CLL involvement, highlighted in color. The volumes (in cubic centimeters) of the axillary (red), intra-abdominal (blue), inguinal (purple) and spleen (green, yellow) disease manifestations are displayed next to each involved area.

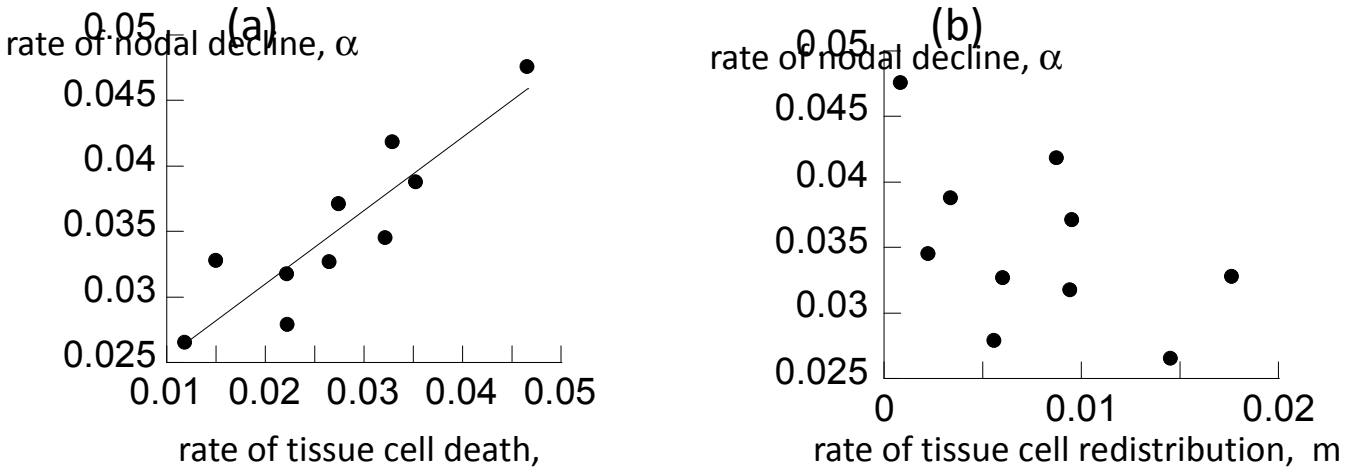

Figure S2 (a) There is a significant correlation between the rate of nodal decline and the death rate of cells in tissue (p=0.0005). (b) There is no significant correlation between the rate of nodal decline and the redistribution rate of CLL cells. The reason is that although both parameters do influence the rate of nodal decline, as defined in $\alpha=d_1+m$, the contribution of the redistribution rate is masked by the dominance of cell death (both parameters vary among patients). For numerical parameter values, see Table 1.